Maintaining phase of the crustacean tri-phasic pyloric rhythm

Christina Mouser* Farzan Nadim† Amitabha Bose ‡

September 10, 2007

Abstract

We construct and analyze a model network of the pyloric rhythm of the crustacean stomatogastric ganglion consisting of an oscillator neuron that inhibits two reciprocally inhibitory follower neurons. We derive analytic expressions that determine the phase of firing of the follower neurons with respect to the oscillator. An important aspect of the model is the inclusion of synapses that exhibit short-term synaptic depression. We show that these type of synapses allow there to be a complicated relationship between the intrinsic properties of the neurons and the synapses between them in determining phase relationships. Our analysis reveals the circumstances and ranges of cycle periods under which these properties work in concert with or independently from one another. In particular, we show that phase maintenance over a range of oscillator periods can be enhanced through the interplay of the two follower neurons if the synapses between these neurons are depressing. Since our model represents the core of the oscillatory pyloric network, the results of our analysis can be compared to experimental data and used to make predications about the biological network.

Keywords: oscillator, phase plane, central pattern generator, synaptic depression

1 Introduction

Neuronal networks responsible for the generation of rhythmic motor activity often operate over a broad range of frequencies [18]. In many such oscillatory central pattern generating (CPG) networks the relative activity phase between groups of neurons remains fixed despite large variations

*Department of Mathematical Sciences, Medgar Evers College of CUNY, Brooklyn, NY 11225: cmouser@mec.cuny.edu

†Department of Mathematical Sciences, New Jersey Institute of Technology, Newark, NJ 07102: farzan@njit.edu

‡Department of Mathematical Sciences, New Jersey Institute of Technology, Newark, NJ 07102: bose@njit.edu

in network frequency [6, 10, 11, 13, 14, 25]. Hence, in face of changes in network frequency, the time delay between the active states of these neuron groups must be adjusted proportionally with the network cycle period. Yet, the biological mechanisms underlying such adjustments are largely unknown. Previous modeling studies have addressed the question of phase determination in neuronal networks. There is a large literature on weakly coupled oscillators (see [8] for example) in which the phase relationship between neurons is obtained through methods of averaging. In studies of the lamprey CPG, the phase between neurons is explicitly constrained within the model [5], allowing the authors to investigate what mechanisms are consistent with the constraint. Work on understanding the inter-segmental lag in the crayfish CPG has focused on the interaction between weak and strong coupling [15, 29].

In previous work, we have suggested that short-term synaptic depression helps promote phase maintenance in feed-forward networks. We showed that depression in the feed-forward inhibitory synapse from an oscillator to a follower neuron allows the phase to be fairly constant over a large range of cycle periods [17] and that intrinsic ionic currents such as the transient potassium A current can act synergistically with synaptic depression to extend the range of phase maintenance [4]. In the current study, we focus on a CPG neuronal network to examine phase maintenance of follower neurons in a three-cell network in which a pacemaker neuron imposes the network oscillations on two follower neurons coupled with reciprocally inhibitory synapses (inset of Fig. 1). The questions of interest center on the synaptic and intrinsic mechanisms that control the activity phase of the follower neurons and their dependence on cycle frequency. This network is modeled after the pyloric network of the crustacean stomatogastric ganglion which consists of an oscillatory pacemaker group of neurons AB and PD and four sets of follower neurons [20]. The pacemaker AB and PD neurons are always co-active, due to strong electrical coupling, and inhibit all follower neurons which, in turn, become active in two distinct (but sometimes overlapping) intervals in each cycle, thus producing a tri-phasic rhythm (Fig. 1A). Previous experimental studies have shown that the activity phases of all neurons in this network are relatively well maintained, despite large variations (0.5-2 Hz) in cycle frequency [13, 14].

In this study, we use the AB neuron as the representative of the pacemaker group and the follower neurons LP and PY as representatives of the follower neurons active in two distinct phases. The other pacemaker neuron type PD two follower neuron types IC and VD, which are co-active with LP and PY, respectively, are not included in our model. Thus, in our model, AB sends feed-forward inhibition to LP and PY while the latter two neurons reciprocally inhibit one another.

We use phase-plane analysis to derive a set of equations that can be numerically solved at any value of the period to determine the phase relationship between AB and the follower neurons. As we vary the cycle period of AB, we investigate how the activity phases of LP and PY changes. The analysis allows us to determine the role of each of the neurons and the synapses between them in setting their activity phases. In particular, we show that when all synapses exhibit short-term depression, there are multiple control mechanisms for setting the phases. These control mechanisms may work in concert or be completely independent from one another. We show that as the cycle period changes, the control of the network phase relationships shifts between different sets of

parameters associated with the neurons and their synapses. Our results, therefore, indicate that synaptic depression within the pyloric network provides a natural mechanism to help the network maintain the observed phase relationships among its different neurons despite large changes in the cycle period.

The mathematical techniques that we employ are motivated by geometric singular perturbation theory in which a difference in time scales is exploited to reduce a high-dimensional model to low-dimensional sub-systems that are more amenable to analysis [21]. We utilize this idea to project the dynamics of the neurons in their silent state onto a two- or three-dimensional phase space. Analyzing the ensuing dynamics in these phase spaces then makes it possible to analytically determine how long each neuron spends in its silent state, thereby allowing us to calculate the phase of each neuron. In parallel, we numerically solve the full set of model equations to see how these numerical solutions compare with those obtained from the analytic reduction method.

The paper is organized as follows. In section 2, we derive the model set of equations and describe the dynamics of synaptic depression. Section 3 contains results with section 3.1 containing the derivation of the firing times and subsequent subsections discussing the role of each of the synapses within the network. Section 4 contains a Discussion in which we address some of the modeling assumptions and implications for the biological network.

2 Model

The network we are studying consists of three neurons, AB, LP, and PY. A schematic of the network architecture is shown in Fig. 1 together with biological and simulation voltage traces of these neurons. AB is the pacemaker neuron of the pyloric network. It oscillates at frequencies that lie between 0.5 and 2.0 Hz [24]. The activity of the pacemaker AB neuron is taken for simplicity to be a square-wave. In particular, we denote the time that AB is active by T_{AB} and the time it is inactive by $T_{inactive}$. Therefore the period of AB satisfies $P = T_{AB} + T_{inactive}$. LP and PY are the follower neurons of the pyloric network. We are mostly interested in the burst envelope of these neurons so we use Morris-Lecar type equations to model their activity [22]. The equations to describe the activity of LP and PY without synaptic connectivity are:

$$\frac{dv_x}{dt} = I_x - g_{leak}[v_x - E_{leak}] - g_{Ca}m_\infty(v_x)[v_x - E_{Ca}] - g_K w_x[v_x - E_K] \quad (1)$$

$$\frac{dw_x}{dt} = \frac{w_\infty(v_x) - w_x}{\tau_{w,x}(v_x)} \quad (2)$$

where x is PY or LP. v_x is the voltage of neuron x, I_x in an applied current, $g_{leak,x}$ is the conductance of the leak current, $E_{leak,x}$ is the reversal potential of the leak current, and w_x is the recovery variable of K^+. The functions m_∞, w_∞, and τ_∞ are sigmoidal functions of voltage and are given in the Appendix. Recent experiments by Rabbah et al [27] showed that the delay in firing of

PY relative to firing of LP is due to intrinsic properties of the neurons. Thus, in the silent state, we choose $\tau_{w,LP}(v_{LP}) < \tau_{w,PY}(v_{PY})$ so that PY has a a slower intrinsic decay rate than LP.

We denote the right-hand side of (1) by $f(v_x, w_x)$. The v_x- and w_x-nullclines associated with (1) and (2) are the set of points $\{(v_x, w_x) : f(v_x, w_x = 0\}$ and $\{(v_x, w_x) : w_x = w_\infty(v_x)\}$. The former is cubic shaped, the latter is sigmoidal. We assume that for both LP and PY, these nullclines intersect at a stable fixed point along the right branch of the cubic nullcline. Thus in the absence of input, both LP and PY tend to a high-voltage fixed point.

LP and PY receive inhibitory synaptic inputs from AB and also from one another. The synapses are modeled to be depressing meaning that the strength of the synapse weakens as the frequency of the pre-synaptic neuron increases. The equations to model the activity of LP and PY are:

$$\frac{dv_{LP}}{dt} = f(v_{LP}, w_{LP}) - \bar{g}_{AB} s_{AB}[v_{LP} - E_{inh}] - \bar{g}_{PY} s_{PY}[v_{LP} - E_{inh}] \quad (3)$$

$$\frac{dw_{LP}}{dt} = \frac{w_\infty(v_{LP}) - w_{LP}}{\tau_{w,LP}(v_{LP})} \quad (4)$$

$$\frac{dv_{PY}}{dt} = f(v_{PY}, w_{PY}) - \bar{g}_{syn,AB} s_{AB}[v_{PY} - E_{inh}] - \bar{g}_{syn,LP} s_{LP}[v_{PY} - E_{inh}] \quad (5)$$

$$\frac{dw_{PY}}{dt} = \frac{w_\infty(v_{PY}) - w_{PY}}{\tau_{w,PY}(v_{PY})} \quad (6)$$

In the above equations, $\bar{g}_{AB}$, $\bar{g}_{PY}$ and $\bar{g}_{LP}$ are the maximal conductances of the AB, PY and LP synapses, respectively, while s_{AB}, s_{PY} and s_{LP} are the associated gating variables. E_{inh} is the reversal potential of the synapses that is chosen so that all synapses are inhibitory.

Our model for the synapses is the same as in [17] where each synapse has a gating variable s_x and another variable d_x that measures the extent of synaptic depression of the synapse. Both variables follow piecewise continuous linear kinetics. They are coupled at discrete moments of time whenever a pre-synaptic cell becomes active. When this occurs, s_x is set equal to the current value

of d_x; see Fig. 2. At all other times the equations for the each of the synaptic variables are:

$$\frac{dd_{AB}}{dt} = \begin{cases} (\hat{d}_{AB}(T_{inactive}) - d_{AB})/\tau_\alpha & v_{AB} \le v_T \\ -d_{AB}/\tau_\beta & v_{AB} > v_T \end{cases} \quad (7)$$

$$\frac{ds_{AB}}{dt} = \begin{cases} -s_{AB}/\tau_\kappa & v_{AB} \le v_T \\ -s_{AB}/\tau_\zeta & v_{AB} > v_T \end{cases} \quad (8)$$

$$\frac{dd_{PY}}{dt} = \begin{cases} (\hat{d}_{PY}(P, T_{PY}) - d_{PY})/\tau_a & v_{PY} \le v_T \\ -d_{PY}/\tau_b & v_{PY} > v_T \end{cases} \quad (9)$$

$$\frac{ds_{PY}}{dt} = \begin{cases} -s_{PY}/\tau_1 & v_{PY} \le v_T \\ -s_{PY}/\tau_2 & v_{PY} > v_T \end{cases} \quad (10)$$

$$\frac{dd_{LP}}{dt} = \begin{cases} (\hat{d}_{LP}(P, T_{LP}) - d_{LP})/\tau_c & v_{LP} \le v_T \\ -d_{LP}/\tau_d & v_{LP} > v_T \end{cases} \quad (11)$$

$$\frac{ds_{LP}}{dt} = \begin{cases} -s_{LP}/\tau_3 & v_{LP} \le v_T \\ -s_{LP}/\tau_4 & v_{LP} > v_T \end{cases} \quad (12)$$

For example, when AB enters its active state, we set $s_{AB} = d_{AB}$ and then let d_{AB} and s_{AB} evolve according to (7) and (8). v_T is the activation threshold of the synapses. When $v_{AB} < v_T$, d_{AB} increases to $\hat{d}_{AB}(T_{inactive})$ (recovery from depression) with rate $1/\tau_\alpha$ where $\hat{d}_{AB}(T_{inactive})$ is an increasing function of $T_{inactive}$ given by

$$\hat{d}_{AB}(T_{inactive}) = (1 + tanh((T_{AB} + T_{inactive} - P_1)/x_1)/2. \quad (13)$$

In this equation, P_1 determines the half-activation time of $\hat{d}_{AB}$ and x_1 determines the steepness of $\hat{d}_{AB}$. This relationship models the dependency of recovery from depression on the cycle period of activity and is used to provide a better approximation of the two time scales of recovery observed in the pyloric synapses [3]. Once v_{AB} goes above threshold (AB becomes active), s_{AB} is set to d_{AB} and then decreases at a rate of $1/\tau_\zeta$ where τ_ζ is a large parameter. While v_{AB} remains above threshold, d_{AB} decreases towards 0 with time constant $1/\tau_\beta$ representing the depression of the AB synapse. Once v_{AB} goes below threshold, s_{AB} decreases to 0 with rate $1/\tau_\kappa$. As the inactive phase of AB increases, the synapse has more time to recover from depression since d_{AB} has more time to increase towards $\hat{d}_{AB}(T_{inactive})$.

Similarly, we let

$$\hat{d}_{LP}(P, T_{LP}) = (1 + tanh((P - T_{LP} - P_2)/x_2))/2, \quad (14)$$

where T_{LP} refers to the length of time LP is inactive. Note that T_{LP} is *a priori* unknown, but will be determined below. $\hat{d}_{PY}(P, T_{PY})$ can also be modeled using a sigmoid similar to $\hat{d}_{AB}$ where T_{PY} refers to the length of time that PY is active. For simplicity, however, we set $\hat{d}_{PY} = 1$.

In some cases that we will examine, the synapses from AB to LP and PY will be non-depressing. In these cases, the strength of the AB synapses will be independent of period. Whenever AB becomes active, we will set $s_{AB} = 1$ instead of d_{AB}.

The mathematical effect of inhibition is to lower the v_x-nullcline of the post-synaptic cell in the (v_x, w_x) phase space. Consider LP for example. Before it receives inhibition from the pacemaker AB, LP lies at a high-voltage fixed point. The inhibition from AB turns on quickly and causes this fixed point to disappear, thereby allowing LP to return to its silent state. Depending on the strength of the AB inhibition (which due to depression is period dependent), the v_{LP}- and w_{LP}-nullclines may intersect either on the middle or left branch of the cubic. In the former case, LP will be able to leave the silent state due to its intrinsic properties, while in the latter LP will remain in the silent state until the AB inhibition decays; Fig. 3 . The general effect of PY inhibition on LP and of AB and LP inhibition on PY is similar.

We will not carry out a formal singular perturbation analysis in this paper. Instead, we will assume that the w_x, s_x and d_x variables evolve more slowly than the v_x variables while the trajectory is away from the branches of a cubic nullcline. This can be achieved by taking the time constants associated with those variables to be large and will allow us to project the dynamics of the neurons while they are near the left branch of a cubic onto a lower dimensional phase space; see [1, 4] for related examples. Simulations of our model are done using the software package XPPAUT [9]. Numerical solutions of equations (25) and (26), below, were obtained using MATLAB. Parameter values are given in the Appendix.

3 Results

We describe the tri-phasic pyloric rhythm starting with the onset of AB activity at $t = 0$ as shown in Fig. 1. AB remains active for time T_{AB} during which time both LP and PY are silent. At $t = t_1$, LP becomes active for a time length T_{LP}. During this time, it inhibits PY. At $t = t_2$, PY becomes active and inhibits LP enough to return LP to the silent state. PY stays active for a time length T_{PY}. After one period $P = T_{AB} + T_{inactive}$, AB again becomes active, inhibiting PY and LP and the cycle continues. We define $\phi_{LP} = t_1/P$ and $\phi_{PY} = t_2/P$ as the phase at which LP and PY fire with respect to the onset of AB activity. The main goal of this paper is to determine these two quantities as a function of P, and to show what effect synaptic depression has on these two phases. Throughout this paper, we shall change P by changing the time $T_{inactive}$ while keeping T_{AB} fixed.

To determine ϕ_{LP} and ϕ_{PY}, we must determine t_1, t_2, T_{LP} and T_{PY}. However the latter two quantities obey $T_{LP} = t_2 - t_1$ and $T_{PY} = P - t_2$. Thus we need only determine two equations for the remaining unknowns t_1 and t_2. To calculate these times we first must understand how LP and PY evolve in their silent state, and what causes them to have a chance to jump to the active state. Consider first LP in the case where only AB inhibition is present. In the $v_{LP} - w_{LP}$ phase plane, inhibition lowers the $v_{LP}-$cubic nullcline. As LP evolves in the silent state, the synapse from AB decays, causing the cubic nullcline to rise slowly back toward its original location. LP can jump to the active state when it reaches a local minimum of any of the slowly rising cubics. These local minima form a one-dimensional LP-jump curve in (v_{LP}, w_{LP}) space; labeled *j.c.* in Fig. 4A. Another way to visualize this is in the (w_{LP}, s_{AB}) phase space; Fig. 4B. When projected into this

phase space, the trajectory moves down and to the left. In addition to the LP-jump curve, there exists a curve of fixed points, labeled $fp.c.$. These points are not true fixed points of the system, but rather are points along which the $v_{LP}-$ and $w_{LP}-$nullclines intersect ($v'_{LP} = w'_{LP} = 0$), but where $s'_{AB} < 0$. A typical trajectory in this phase space will transition to the active state when it reaches the jump curve. Let us now add in the PY inhibition to LP. In this case, LP must potentially wait for both the AB and PY inhibitions to decay in order to jump to the active state. The local minima of the associated cubics now form a two-dimensional jump surface ($j.s.$) and the fixed points form a two-dimensional surface ($fp.s.$) as shown in the (w_{LP}, s_{AB}, s_{PY}) phase space in Fig. 4C. Similarly, there exists a two-dimensional PY-jump surface resulting from the slow decay of the AB and LP synapses to PY and a two-dimensional surface of fixed points.

Let us assume that AB becomes active at $t = 0$ and that both LP and PY are in their silent state. LP is the first to reach its jump surface, primarily because of the assumption that when the neurons are below threshold, $\tau_{w,LP}(v_{LP}) < \tau_{w,PY}(v_{PY})$. Assume that the jump surface is a plane and can be expressed by the linear relationship:

$$\bar{g}_{AB}s_{AB} + \bar{g}_{PY}s_{PY} + M_1 w_{LP} = g^*_{syn1}. \tag{15}$$

Note that if $\bar{g}_{PY} = 0$, (15) reduces to the equation for a one-dimensional linear jump curve as in [4]. The constants M_1 and g^*_{syn1} are both positive and can be determined from the $\bar{g}_{PY} = 0$ case. The former is related to the slope of the LP-jump curve; the latter is related to the level of inhibitory synaptic input needed to make the v_{LP}-nullcline tangent to the w_{LP}-nullcline; see figure 4B. We now calculate the value at time t_1 of the three dynamic variables explicitly represented in (15). The first is the easiest. Since AB is taken to be a periodic square wave function (with period $P = T_{AB} + T_{inactive}$), the value of the depression variable d_{AB} will also be periodic. Using this fact, it is straightforward to find that the maximal value of d_{AB} occurs at the onset of AB activity and is given by

$$d_{max,AB}(P) = \hat{d}_{AB}(T_{inactive})\frac{[1 - e^{-T_{inactive}/\tau_\alpha}]}{1 - e^{-T_{AB}/\tau_\beta}e^{-T_{inactive}/\tau_\alpha}}. \tag{16}$$

Note that $d_{max,AB}(P)$ is an increasing function of $T_{inactive}$. At the time that AB becomes active s_{AB} is set equal to $d_{max,AB}$ and then decays according to (8). Thus $s_{AB}(T_{AB}) = d_{max,AB}(P)e^{-T_{AB}/\tau_\zeta}$. During the time that AB is silent, s_{AB} decays with time constant τ_κ, so

$$s_{AB}(t_1) = d_{max,AB}(P)e^{-T_{AB}/\tau_\zeta}e^{-(t_1 - T_{AB})/\tau_\kappa}. \tag{17}$$

Note that the case when AB is not depressing can be considered by simply setting $d_{max,AB} \equiv 1$. We next calculate $s_{PY}(t_1)$. Since the tri-phasic rhythm is assumed to be periodic, we similarly find that

$$d_{max,PY}(P, T_{PY}) = \frac{[1 - e^{-(P - T_{PY})/\tau_a}]}{1 - e^{-T_{PY}/\tau_b}e^{-(P - T_{PY})/\tau_a}}. \tag{18}$$

This maximum occurs at the onset of the PY burst. Note that $d_{max,PY}$ depends on T_{PY} where this term is to be determined by t_2 ($T_{PY} = P - t_2$). Utilizing the activity of the previous cycle of a periodic solution, $t = 0$ corresponds to the end of a PY burst. Therefore $s_{PY}(0) = d_{max,PY}e^{-T_{PY}/\tau_2}$ and at time t_1

$$s_{PY}(t_1) = d_{max,PY}(P, T_{PY})e^{-T_{PY}/\tau_2}e^{-t_1/\tau_1}. \tag{19}$$

Finally, we determine $w_{LP}(t_1)$. When PY becomes active (during the previous cycle) assuming $\bar{g}_{PY} > 0$, LP returns to the silent state with a value we denote $\hat{w}_{LP}$. LP stays in the silent state for time $T_{PY} + t_1 = P - (t_2 - t_1)$. Assuming that $w_\infty(LP) \approx 0$ near the left branches of the v_{LP} nullcline and that $\tau_{w,LP}(v_{LP})$ is a constant denoted by $\tau_{w,LP}$, we find

$$w_{LP}(t_1) = \hat{w}_{LP}e^{-(P-(t_2-t_1))/\tau_{w,LP}}. \tag{20}$$

We can now substitute equations (17)-(20) into (15). Note however that if $\bar{g}_{PY} = 0$, then LP stays in the active state until AB becomes active and (20) is replaced by $w_{LP}(t_1) = \hat{w}_{LP}e^{-t_1/\tau_{w,LP}}$.

To find a second equation relating the times t_1 and t_2, we use a linear approximation for the PY-jump surface:

$$\bar{g}_{AB}s_{AB} + \bar{g}_{LP}s_{LP} + M_2 w_{PY} = g^*_{syn2}. \tag{21}$$

Similar to before,

$$s_{AB}(t_2) = d_{max,AB}(P)e^{-T_{AB}/\tau_\zeta}e^{-(t_2-T_{AB})/\tau_\kappa}. \tag{22}$$

To calculate $s_{LP}(t_2)$, we note that LP becomes active at $t = t_1$. Thus independent of the value of s_{LP} prior to t_1, $s_{LP}(t_1) = d_{max,LP}$, where

$$d_{max,LP}(P, T_{LP}) = \hat{d}_{LP}(P, T_{LP})\frac{[1 - e^{-(P-T_{LP})/\tau_c}]}{1 - e^{-T_{LP}/\tau_d}e^{-(P-T_{LP})/\tau_c}}. \tag{23}$$

LP remains active until time t_2 which implies

$$s_{LP}(t_2) = d_{max,LP}e^{-(t_2-t_1)/\tau_4}. \tag{24}$$

Similar to before $w_{PY}(t_2) = \hat{w}_{PY}\exp(-t_2/\tau_{w,PY})$ where $\tau_{w,PY}$ is the time constant for PY activity in its silent state. We can now substitute into (21) to obtain the following two equations for t_1 and t_2:

$$\begin{aligned}&\bar{g}_{AB}d_{max,AB}(P)e^{-T_{AB}/\tau_\zeta}e^{-(t_1-T_{AB})/\tau_\kappa} + \bar{g}_{PY}d_{max,PY}(P, T_{PY})e^{-T_{PY}/\tau_2}e^{-t_1/\tau_1} \\ &+ M_1\hat{w}_{LP}e^{-(P-T_{LP}))/\tau_{w,LP}} = g^*_{syn1}.\end{aligned} \tag{25}$$

$$\begin{aligned}&\bar{g}_{AB}d_{max,AB}(P)e^{-T_{AB}/\tau_\zeta}e^{-(t_2-T_{AB})/\tau_\kappa} + \bar{g}_{LP}d_{max,LP}(P, T_{LP})e^{-T_{LP}/\tau_4} \\ &+ M_2\hat{w}_{PY}e^{-t_2/\tau_{w,PY}} = g^*_{syn2}.\end{aligned} \tag{26}$$

Note that $T_{PY} = P - t_2$, and if $\bar{g}_{PY} = 0$ then $T_{LP} = P - t_1$, while if $\bar{g}_{PY} > 0$ then $T_{LP} = t_2 - t_1$.

Equations (25) and (26) can be solved numerically to obtain t_1 and t_2. In specific parameter regimes, certain terms on the left-hand side of the above equations become small and an analytic estimate for t_1 and t_2 becomes possible. Our goal for the remainder of the paper is to use (25) and (26) to understand how $\phi_{LP} = t_1/P$ and $\phi_{PY} = t_2/P$ depend on the parameters in these equations. We shall check this for several cases; when the LP and PY inhibition is absent (section 3.1), when LP to PY inhibition is added (section 3.2), when PY to LP inhibition is present (section 3.3), and when both reciprocal synapses are present (section 3.4).

3.1 Phase determination with no synapses between LP and PY

When the synapses between LP and PY are removed, we set $\bar{g}_{LP} = 0$ and $\bar{g}_{PY} = 0$ in equations (25) and (26). Then t_1 and t_2 (and, therefore ϕ_{LP} and ϕ_{PY}) are determined by the properties of the AB synapses and the intrinsic properties of the neurons. In this case, the dependence of ϕ_{LP} on P has been previously shown by Manor et al [17], and that of ϕ_{PY} is similar.

If the AB synapses onto LP and PY are not depressing, then ϕ_{LP} and ϕ_{PY} both decay like $1/P$ since (25) and (26) are no longer period dependent. For each cell, this decay is controlled either by τ_κ the time constant of decay of the AB synapses and $\bar{g}_{AB}$ the maximal conductance of the synapse or by the cell's own intrinsic time constant of decay in the silent state, $\tau_{w,LP}$ or $\tau_{w,PY}$. The situation changes dramatically when the AB synapses are depressing. Following the results of Manor et al [17], with an appropriate choice of parameters, both sets of parameters can control the phase curves, each doing so at different ranges of periods. In particular, when τ_κ is large enough so that the synaptic decay is slower than the rate at which w_{PY} and w_{LP} decay on the left branches of their respective nullclines, phase maintenance is enhanced. In Fig. 5A, we can see that for $500 < P < 650$, ϕ_{LP} and ϕ_{PY} decrease. In this range of periods, the synapses from AB to LP and PY are largely depressed and, consequently, do not significantly contribute to the time at which LP and PY fire. Here the first terms on the left-hand sides of (25) and (26) are close to zero, the second terms are absent ($\bar{g}_{PY} = \bar{g}_{LP} = 0$) and therefore the third terms alone determine t_1 and t_2. Thus in this range, phase is mostly determined by the intrinsic dynamics of LP and PY. In the range $650 < P < 1000$, the AB synapse increasingly recovers from depression ($d_{max,AB}$ gets larger; Fig 5B). As a result the synaptic properties take over control for setting ϕ_{LP} and ϕ_{PY} in this range. For $P > 1000$, the AB synapse has maximally recovered from depression causing $d_{max,AB}$ to saturate. Now the first terms on the left-hand sides of (25) and (26) take longer to decay then the third terms (since τ_κ is large enough). Thus the synapses from AB determine the firing times. However, as the period increases, the phase decreases like $1/P$ since the value of $d_{max,AB}$ in the first terms will eventually saturate; $d_{max,AB} \to 1$ as $P \to \infty$ [17]. These three regimes combine together to cause the phase curve to be cubic in shape. Thus, although a constant phase is not perfectly achieved, phase-maintenance is better than when the AB synapse is non-depressing where ϕ_{LP} and ϕ_{PY} decay like $1/P$.

3.2 The effect of LP to PY inhibition on ϕ_{PY}

We now explore how the presence of the LP to PY synapse affects ϕ_{PY}. We show that the inclusion of the LP to PY synapse leads to another way to control the phase of PY activity. In (25) and (26), we let $\bar{g}_{PY} = 0$ while setting $\bar{g}_{LP}$ to a positive value. When the synapse from LP to PY is present, each time LP is active, it provides further inhibition to PY. In order for PY to fire, the LP inhibition must also decay. Therefore, the additional time it now takes for PY to fire is determined, in part, by the the size of $\bar{g}_{LP}s_{LP}$ and the rate at which s_{LP} decays. Using equation (26), we can determine over which parameter regimes the LP to PY synapse significantly contributes to ϕ_{PY}. For example, suppose τ_4, the time constant of decay of the s_{LP} synapse when LP is active, is small enough, or that $\bar{g}_{LP}$, the maximal conductance of this synapse is small. Then the term $\bar{g}_{LP}s_{LP}$ is insignificant and, therefore the LP to PY synapse does not significantly affect t_2. However, if τ_4 is not so small compared with τ_κ and $\tau_{w,PY}$, and if $\bar{g}_{LP}$ is big enough, then the LP inhibition will more significantly contribute to ϕ_{PY}.

The period dependence of the LP synapse and the rates of depression and recovery also play a role in setting phase. For example if the time constant of recovery from depression of the LP synapse (τ_c) is very small, then the synapse will recover quickly and will largely be period independent. Similarly, if the depression time constant τ_d is small, then the synapse will be ineffective at suppressing its post-synaptic target. More interestingly, depending on the value of parameters, the the LP to PY synapse can work in concert with or independently of the AB synapse to effect PY firing. Figure 6A shows graphs of the ϕ_{LP}, ϕ_{PY} and $d_{max,LP}$ for different choices of the parameter P_2, the half activation of the strength of the LP to PY. The dashed line traces show the case when $P_2 = 570$ (note the half-activation of the AB synapse $P_1 = 870$ in all cases), the dotted line traces when $P_2 = 870$ and the solid traces when $P_2 = 1770$. In the latter case, the length of the LP interburst ($t_1 = P - T_{LP}$) never becomes large enough to cause the LP to PY synapse to gain strength. Thus $d_{max,LP} = 0$ (Fig. 6B) and ϕ_{PY} looks as it would if $\bar{g}_{LP} = 0$. When the parameter P_2 is lowered to 870, then the LP to PY synapse does strengthen around $P = 1380$ (dotted traces) because $P - T_{LP}$ becomes larger than P_2. Here, the synapse becomes strong in a range of periods for which the AB synapse is already saturated. Thus it controls ϕ_{PY} quite independently of the AB to PY synapse. When, $P_2 = 190$ (dashed traces), the LP to PY synapse works in concert with the AB to PY synapse to delay PY firing. Here the phase curve has a single local maximum that is larger in value than when the LP to PY synapse is absent. Numerical simulations of the full set of equations using XPPAUT yield similar results (not shown). As $P \to \infty$, the value of $d_{max,LP}$ tends to $\hat{d}_{LP}[1 - \exp(-(P - T_{LP})/\tau_c)]$ since $T_{LP} \to \infty$ as can be seen from equations (14) and (23). Thus $d_{max,LP}$ is bounded away from one and thus the LP to PY synapse never fully recovers.

3.3 The role of PY to LP inhibition on ϕ_{LP} and ϕ_{PY}

Next we address what effect the synapse from PY to LP has on the phase of LP and PY. Again depending on the parameters, there are many possibilities that can be considered. However we

shall take a cue from the biological system and study one important subcase. It is known that the PY to LP synapse is initially strong, depresses very quickly and also decays very quickly once PY becomes silent [16]. From these results, we conclude that the primary role of the PY to LP synapse is to end the firing of LP and return it to its active state. This simple role, however, has a dramatic affect on both ϕ_{LP} and ϕ_{PY}. First, the knocking down of LP to its silent state by PY means that at small periods, ϕ_{LP} decreases. In particular, for small values of P, the AB synapse is weak and does not play a big role in setting t_1, which is set mainly by the intrinsic properties of LP. Once LP is on the left branches of its v_{LP} nullcline, w_{LP} begins to decay before AB becomes active. Thus when AB next becomes active, LP is much closer to the jump surface than it would have been had it been knocked down to the silent state by AB, Fig. 7. Thus the remaining time that LP must now spend evolving toward the jump surface is much smaller in the presence of the PY synapse than in its absence. Therefore t_1 is significantly smaller and ϕ_{LP} decreases. At large P, however, the AB synapse is stronger and continues to dominate the determination of t_1. This is especially true if we choose τ_1, the time constant of decay of the PY to LP inhibition to be small.

The second effect of the presence of the PY to LP synapse is to strengthen the LP to PY synapse. This is because the presence of the PY to LP synapse causes LP to have a shorter active duration than when this synapse is absent. Note that when $\bar{g}_{PY} = 0$ (the PY to LP inhibition is absent), $T_{LP} = P - t_1$, whereas when $\bar{g}_{PY} > 0$ (the PY to LP inhibition is present), $T_{LP} = t_2 - t_1$ because the PY inhibition ends the LP burst. Thus LP spends a larger fraction of its period in the silent state, which, in turn increases both terms of equation (23) allowing $d_{max,LP}$ to increase with P, Fig. 8. Moreover, since T_{LP} is bounded as $P \to \infty$, $d_{max,LP} \to 1$ in this limit. Therefore independent of the value of P_2, the LP to PY synapse will play a role in setting the PY phase. Thus, the effect of PY inhibition is to strengthen the inhibition that it itself receives! The ramifications of this are explored in the next section.

3.4 Reciprocal inhibition between LP and PY

The above results indicate that the inhibitory synapses between the two pyloric neurons LP and PY can play a role in enhancing the ability of the neurons to achieve phase maintenance. Indeed, we have seen that the LP to PY synapse can control PY phase in a range of periods for which the AB synapses to LP and PY are already saturated, and thus are no longer period dependent. Therefore, it is natural to consider cases in which the AB inhibition is both non-depressing and depressing.

When the AB synapse is non-depressing ($d_{max,AB} \equiv 1$), and the inhibition between LP and PY is absent, ϕ_{LP} and ϕ_{PY} decrease like $1/P$. In order for the synapse from LP to PY to be able to create a range of periods over which ϕ_{PY} increases, d_{LP} must increase as the period increases. Similarly, d_{PY} must increase as the period increases in order to create a range of periods over which ϕ_{LP} increases. Let us first consider $d_{max,LP}$ as given by equation (23). This term will increase as period increases so long as LP spends increasingly longer times in the silent state. As P increases, even though the time t_1 need not increase the time $P - T_{LP}$ will. To understand this, recall that

one role of the PY inhibition to LP is to return the latter to the silent state at an earlier stage than AB would have. This is independent of depression of either the AB or PY synapses. Thus the LP to PY synapse will have a chance to recover for more time and thereby will strengthen. A stronger LP to PY synapse delays PY firing and thus increases ϕ_{PY}. In Fig 9A, we show an example of this; panel A1 is obtained by solving the full set of equations numerically with XPPAUT, while panel A2 is obtained by solving (25) and (26) with MATLAB. In particular, the LP to PY synapse becomes strong when $P - T_{LP} > P_2 (= 1140)$. In this range, the value of the synaptic and depression time constants associated with the LP synapse play an increasingly larger role in setting PY phase. If the time constant of LP to PY synaptic decay is chosen to be large relative to the time constant of decay of the AB synapse, then the LP synapse can increase the phase of PY for a range of periods larger than P_2. For very large values of P, the LP synapse will fully recover from depression and will not be able to further increase the delay of PY firing. Thus for large P, we expect ϕ_{PY} to decay like $1/P$ as shown in the figure.

A delay in PY firing has the added effect of strengthening the PY to LP synapse provided that this synapse is also depressing, as PY spends more time in the silent phase. This can have a very subtle effect on the LP phase. At first glance, the PY to LP synapse does not appear to do much to help LP phase be constant, instead almost all of this work falls on AB. However PY does put LP in a position so that at small periods, the intrinsic controlled LP phase is much closer to the larger period AB-synaptically controlled LP phase. Moreover at these larger periods where the AB synapse is strengthening, increases in strength of the PY to LP synapse can induce changes in the LP phase. This is because this synapse can now complement the AB to LP synapse to keep the LP neuron near the jump surface for a longer time, thereby delaying LP firing. This subtle effect, however, does not dramatically affect the LP phase since the time constant of decay of the PY to LP synapse is small. Thus its effect will have worn off by the next LP cycle. This is consistent with the biological system where the PY to LP synapse is a strong, short lasting one whose main effect is to terminate LP firing [16].

In summary, when the AB input is non-depressing, the depression of the LP to PY synapse can still be utilized to improve phase maintenance of PY. However the phase of LP is still mostly determined by the AB synapse and basically decays like $1/P$.

When the reciprocal inhibition between LP and PY is present and the AB synapses are depressing, the complexity of the network is increased. However, the dynamics of LP and PY can be understood based on the results of sections 3.1-3.3. As discussed above, depending on parameters, various synaptic or intrinsic parameters play a role in setting phase at different intervals of period. Let us focus on the case where $P_2 > P_1$ ($P_2 = 1470$ and $P_1 = 870$). In this case, both ϕ_{LP} and ϕ_{PY} can have several local maxima and minima and, in particular, can have good phase maintenance over a large range of periods. Figure 9B shows one such case where ϕ_{LP} varies between .35 and .45 and ϕ_{PY} varies between .6 and .7 for $P \in [500, 2400]$. These curves can be parsed into three distinct intervals. At small periods, the AB, LP and PY synapses are weak and play little role in setting phase. Here intrinsic parameters of LP and PY, namely $\tau_{w,LP}$ and $\tau_{w,PY}$, are more important; only the last term of the left hand side of equations (25) and (26) is large. At intermediate periods, the

AB synapse strengthens while the LP and PY synapses remain weak. Here, the time constant of AB synaptic decay, τ_κ, is the most important parameter in setting phase. The first term on the left hand side of (25) and (26) is dominant. Finally, at larger P, the AB synapse has saturated and plays no additional role in setting phase. Instead, at these periods the LP and PY synapses have strengthened enough to be important. In particular, the inhibition from PY to LP allows LP to spend more time in the silent state, thereby strengthening the LP to PY synapse. This strengthened synapse in turn delays PY firing, increasing its phase, and strengthening the PY to LP synapse. The time constants of decay between the LP and PY reciprocal synapses play the most important role of setting phase for large P. In this case, the first and second terms on the left hand side of (25) and (26) are large, but the first terms decay more quickly then the second terms. Thus the control of phase for large P is most strongly controlled by time constants associated with the reciprocal LP and PY synapses.

The importance of the PY to LP synapse in redirecting the role of the LP to PY synapse can not be overstated. In particular, when the PY to LP synapse is absent, the LP to PY synapse strengthens only as a result of the effect of the delay to firing induced by the AB to LP synapse. The LP to PY synapse is only effective in a range of periods that depends closely on the AB to LP synapse; see section 3.2 and the relationship between the parameters P_1 and P_2. However, when the PY to LP synapse is present, the LP to PY synapse can act much more independently. Namely, it can strengthen in a range of periods that is largely independent of any effects of the AB induced delay, and therefore can affect the PY phase curve in a range of periods that is different than the AB synapse does. In particular, in order for the LP synapse to strengthen, the value of P_2, the half-activation of the depression and recovery term associated with d_{LP} need not be related to P_1, the half-activation associated with d_{AB}.

4 Discussion

Central pattern generating (CPG) networks are often driven by pacemaker neurons that set the network frequency and the influence the firing times of follower neurons via feed-forward synapses [7]. Nonetheless, the dynamics of these networks are often modulated or controlled by mechanisms that are downstream from the feed-forward inputs. Even in small networks, the dynamics resulting from the interactions among the rhythmically active neurons can be surprisingly complicated. We have analyzed a simplified network, modeling the pyloric CPG of the crustacean stomatogastric ganglion. Our results build on our previous studies that examined the effect of short-term synaptic depression, a common property of many synapses, on the activity phase of a follower neuron in a two-cell feed-forward network [4, 17].

In this study we focused on a three-cell network, consisting of a pacemaker neuron AB that produces feed-forward inhibitory synapses on two follower neurons LP and PY. The follower neurons also have reciprocally-inhibitory synaptic connections thus producing feedback interactions in the network. We examined the mechanisms that determine the activity phase of LP and PY in

face of changes in network frequency. Our analysis demonstrates that phase constancy is enhanced when the synapses between neurons are depressing. As a result, the PY and LP neurons can keep a relatively constant phase over a four-fold change in the network cycle period, consistent with the experimental findings of Hooper [13].

Mathematical analysis carried out in lower dimensional phase spaces allowed us to understand how different combinations of parameters can affect the activity phase of follower neurons in different ranges of the cycle period. It also revealed a number of interesting facts about how the dynamics of the network evolve. For example, it has traditionally been thought that the primary role of the PY to LP synapse is simply to return LP to its silent state [27]. Our analysis now demonstrates that an additional effect of this synapse is to strengthen the LP to PY synapse by causing LP to spend more time in its silent state, allowing for recovery from short-term depression. This effect occurs whether or not the PY to LP synapse is depressing, thus indicating that the plasticity of this synapse may not be so critical to the proper functioning of the network.

4.1 Role of synaptic depression

Many synaptic connections in CPGs exhibit short-term depression [19, 23, 26]. Our results show that synaptic depression can play a variety of potential roles in setting the phases of the follower LP and PY neurons. First, the feed-forward synapses from AB to both LP and PY allow the intrinsic properties of these follower neurons to determine phase at small periods where the AB synapses are weak. At intermediate cycle periods, these same synapses strengthen and become more effective in the control of the activity phases. Second, the depression in the LP to PY synapse allows the PY phase to be determined by this synapse in different ranges of periods. If the LP synapse strengthens in the same range of periods as the AB synapses, then these two work in concert to determine PY phase. If not, the LP to PY synapse can work independently of the AB to PY synapse to influence the phase of PY activity. As a consequence, even if the AB synapse is non-depressing, the LP to PY synapse can still promote phase constancy of ϕ_{PY} (to be better than $1/P$) in some range of periods. Third, as shown in section 3.4, depression in the PY to LP synapse can also have a small but subtle effect on the LP phase. Thus, changes in the cycle period of the pacemaker neuron AB may not directly affect AB's synapses, yet result in changes in downstream synapses that the pacemaker does not directly target. This provides another set of candidate mechanisms that can affect the phase of the follower neurons.

4.2 Consequences of model assumptions

The primary modeling assumption made here is that the individual spikes within a burst are not of large relevance in determining the phase relationships of neurons. Synapses in the stomatogastric ganglion have both a spike-mediated and a non-spike-mediated (graded) component whose strength depends on the slow oscillatory waveforms of the presynaptic neuron [12]. When action potentials,

and therefore spike-mediated transmission, is blocked by bath application of tetrodotoxin, a triphasic rhythm characteristic of the pyloric network activity can be generated by applying various modulatory substances [2]. Thus, the simplified Morris-Lecar type models and graded synapses used provide a good first-order approximation of the activity of the pyloric network, in particular the envelope of the slow oscillations (as in Fig. 1) and its underlying synaptic mechanisms.

The other major modeling assumption is that the jump surfaces in the silent states of LP and PY are planes. This assumption allowed us to analytically derive (25) and (26). The results shown in Fig. 9 validate this assumption as they show a very good qualitative agreement between phase curves obtained from (25) and (26) with those obtained by numerically solving the full set of equations. This qualitative agreement occurs despite the fact that our analytic reduction effectively ignores the behavior of the neurons when they are active and only records their w values at the moment they return to the silent state.

4.3 Conclusions

Many neural networks maintain a constant relative phase in the activity patterns of participating neurons despite changes in network frequency [6, 25]. In CPGs this constraint on phase is of special importance because the underlying neural patterns are commanded to muscles that often have to be activated at precise phases of each cycle in order to produce meaningful behavior, for example, locomotion [28, 29]. We have built on our previous modeling results to propose mechanisms through which synaptic dynamics, such as short-term depression, can contribute to phase maintenance in face of changes in network frequency. Our most important findings are that synaptic interactions among follower neurons may affect their phase in each cycle of oscillation and that these interactions may extend the range of cycle periods for which there is phase maintenance beyond those made possible by the dynamics of the feed-forward synapses from the pacemaker neurons. These predictions are potentially important for understanding mechanisms underlying phase maintenance in the pyloric network and can be experimentally tested by manipulating the strength and dynamics of the synapses in this network using pharmacological agents or the dynamic clamp technique.

5 Appendix

We numerically solved equations (1)-(14) to obtain our results. In these equations $m_\infty(v_x) = 0.5(1+tanh((v_x+1.2)/18))$, $w_\infty(v_x) = 0.5(1+tanh((v_x-15)/5))$, and $\tau_w(v_x) = m_x(40-30w_\infty(v_x))$. For both LP and PY, $I_x = 75$, $g_{leak} = 2$, $E_{leak} = -60$, $E_{inh} = -80$, $g_{Ca} = 4$, $E_{Ca} = 120$, $g_K = 8$, and $E_K = -84$. In all simulations, $T_{AB} = 300$, $\tau_\alpha = 1800$, and $\tau_\beta = 15$.

In the case of the depressing synaptic AB input, $m_{LP} = 8.1$, $m_{PY} = 8.4$ and $\bar{g}_{AB} = 1.8$. When the LP and PY synaptic inputs were present, we set $\bar{g}_{LP} = 1$ and $\bar{g}_{PY} = 2$. However, when these synapses were not present, $\bar{g}_{LP}$ and $\bar{g}_{PY}$ were set equal to 0. The remaining parameter values were

as follows : $\tau_\kappa = 1650$, $\tau_c = 3300$, $\tau_d = 990$, $\tau_a = 2700$, $\tau_b = 150$, $\tau_1 = 60$, $\tau_2 = 600$, $\tau_3 = 210$, $\tau_4 = 300$, $x_1 = 55$, $x_2 = 35$, $P_1 = 570$ and $P_2 = 1470$.

When the AB synapses were not depressing, we simply set $d_{AB} \equiv 0.38$. We changed $m_{LP} = 2.55$, $m_{PY} = 3.15$, $\bar{g}_{AB} = 1.4$, $\bar{g}_{LP} = 13$, $\bar{g}_{PY} = 11$, $\tau_\kappa = 1200$, $\tau_c = 60$, $\tau_d = 60$, $\tau_a = 1350$, $\tau_b = 240$, $\tau_1 = 60$, $\tau_2 = 1350$, $\tau_3 = 330$, $\tau_4 = 60$, $P_2 = 1140$ and $x_2 = 10$.

We solved equations (25) and (26) using MATLAB. We used the same set of parameter values as we did when using XPPAUT. There are a few parameters in these equations that do not explicitly appear in (1)-(14) that can be estimated from the geometry of the nullclines. We set $M_1 = M_2 = 3.12$, $\hat{w}_{LP} = \hat{w}_{PY} = 1$. For the non-depressing case Fig. 9 A1 and A2, $g^*_{syn1} = 2$, $g^*_{syn2} = 1.5$, $\tau_{w,LP} = 102$, $\tau_{w,PY} = 126$, and for the depressing case Fig. 9, B1 and B2, $g^*_{syn1} = 1.05$, $g^*_{syn2} = 1$, $\tau_{w,LP} = 240$, $\tau_{w,PY} = 255$.

Acknowledgments: This work was supported, in part, by a grant from The City University of New York PSC-CUNY Research Award Program (CM), the National Science Foundation DMS-0315862 (AB, CM) and DMS-0615168 (AB) and the National Institutes of Health MH-60605 (FN).

References

[1] Ambrosio-Mouser, C., Nadim, F. and Bose, A. *The effects of varying the timing of inputs on a neural oscillator*, SIAM J. Appl. Dyn. Syst., 5 (2006), 108-139.

[2] Anderson, W.W., Barker, D.L. *Synaptic mechanisms that generate network oscillations in the absence of discrete postsynaptic potentials.* J. Exp. Zool. 216 (1981), 187-191.

[3] Birmingham, J.T., Manor, Y., Nadim, F., Abbott, L.F., and Marder, E. *An empirical model describing the dynamics of graded synaptic transmission in the lobster pyloric network* In Computational Neuroscience: Trends in Research, (1998), James M. Bower ed. (Plenum Press, NY).

[4] Bose, A., Manor, Y. and Nadim, F. *The activity phase of postsynaptic neurons in a simplified rhythmic network*, J. Comput. Neurosci., 17 (2004), 245-261.

[5] Cohen, A., Ermentrout, G.B., Kiemel, T., Kopell, N., Sigvardt, K. and Williams, T. *Modelling of intersegmental coordination in the lamprey central pattern generator for locomotion*, TINS, 15 (1992), 434-438.

[6] DiCaprio, R.A., Jordan, G., Hampton, T. *Maintenance of motor pattern phase relationships in the ventilatory system of the crab.* J. Exp. Biol., 200 (1997), 963-974.

[7] Dickinson P.S. *Neuromodulation of central pattern generators in invertebrates and vertebrates.* Curr. Opin. Neurobiol., 16 (2006), 604-614.

[8] Ermentrout, G.B. *n:m phase-locking of weakly coupled oscillators*, J. Math. Biol., 12 (1981), 327-342.

[9] Ermentrout, G.B. *Simulating, analyzing, and animating dynamical systems: A guide to XPPAUT for researchers and students*, SIAM, 2002.

[10] Friesen, W.O. and Pearce, R.A. *Mechanisms of intersegmental coordination in leech locomotion.* Sem. Neurosci., 5 (1993), 41-47.

[11] Grillner, S. *Control of locomotion in bipeds, tetrapods and fish.* In: Handbook of Physiology, section 1, The Nervous system, vol II (V.B. B, ed), (1981) 1179-1236. Maryland: Waverly Press.

[12] Graubard, K., Raper, J.A., Hartline, D.K. *Graded synaptic transmission between identified spiking neurons* J. Neurophysiol. 50 (1983), 508-521.

[13] Hooper, S. *Phase maintenance in the pyloric pattern of the lobster (Panulirus interruptus) stomatogastric ganglion*, J. Comput. Neurosci., 4 (1997), 191-205.

[14] Hooper, S. *The pyloric pattern of the lobster (Panulirus interruptus) stomatogastric ganglion comprises two phase-maintaining subsets*, J. Comput. Neurosci., 4 (1997), 207-219.

[15] Jones, S. and Kopell, N. *Local network parameters can affect inter-network phase lags in central pattern generators*, J. Math. Biol. 52 (2006), 115-40.

[16] Mamiya, A., Manor, Y. and Nadim, F. *Short-term dynamics of a mixed chemical and electrical synapse in a rhythmic network*, J. Neurosci., 23 (2003), 9957-9564.

[17] Manor, Y., Bose, A., Booth, V. and Nadim, F. *Contribution of synaptic depression to phase maintenance in a model rhythmic network*, J. Neurophysiol., 90 (2003), 3513-3528.

[18] Marder, E. and Calabrese, R. *Principles of rhythmic motor pattern generation*, Physiol. Rev. 76 (1996), 687-717.

[19] Marder, E. *From biophysics to models of network function*, Annu. Rev. Neurosci., 21 (1998), 25-45.

[20] Marder, E., Bucher, D. *Understanding circuit dynamics using the stomatogastric nervous system of lobsters and crabs.* Annu. Rev. Physiol., 69 (2006) 291-316.

[21] Mishchenko, E.F., Rozov, N.K., *Differential Equations with Small Parameters and Relaxation Oscillators.* (1980) New York: Plenum Press.

[22] Morris, C. and Lecar, H. *Voltage oscillations in the barnacle giant muscle fiber*, Biophys. J., 35 (1981), 193-213.

[23] Nadim, F., Manor, Y. Kopell, N. and Marder, E. *Synaptic depression creates a switch that controls the frequency of an oscillatory circuit*, PNAS, 96 (1999), 8206-8211.

[24] Nusbaum, M.P. and Beenhakker, M.P. *A small-systems approach to motor pattern generation*, Nature, 417 (2002), 343-50.

[25] O'Keefe, J., Recce, M.L. *Phase relationship between hippocampal place units and the EEG theta rhythm.* Hippocampus, 3 (1993) 317-330.

[26] Parker, D. and Grillner, S. *Activity-dependent metaplasticity of inhibitory and excitatory synaptic transmission in the lamprey spinal cord locomotor network*, J. Neurosci., 19 (1999), 1647-1656.

[27] Rabbah, P. and Nadim, F. *Synaptic dynamics do not determine proper phase of activity in a central pattern generator*, J. Neurosci., 25 (2005), 11269-11278.

[28] Sigvardt, K. A.*Spinal mechanisms in the control of lamprey swimming.* Am. Zool. 29 (1981) 19-35.

[29] Skinner, F. and Mulloney, B. *Intersegmental coordination of limb movements during locomotion: Mathematical models predict circuits that drive swimmeret beating*, J. Neurosci., 18 (1998) 3831-3842.

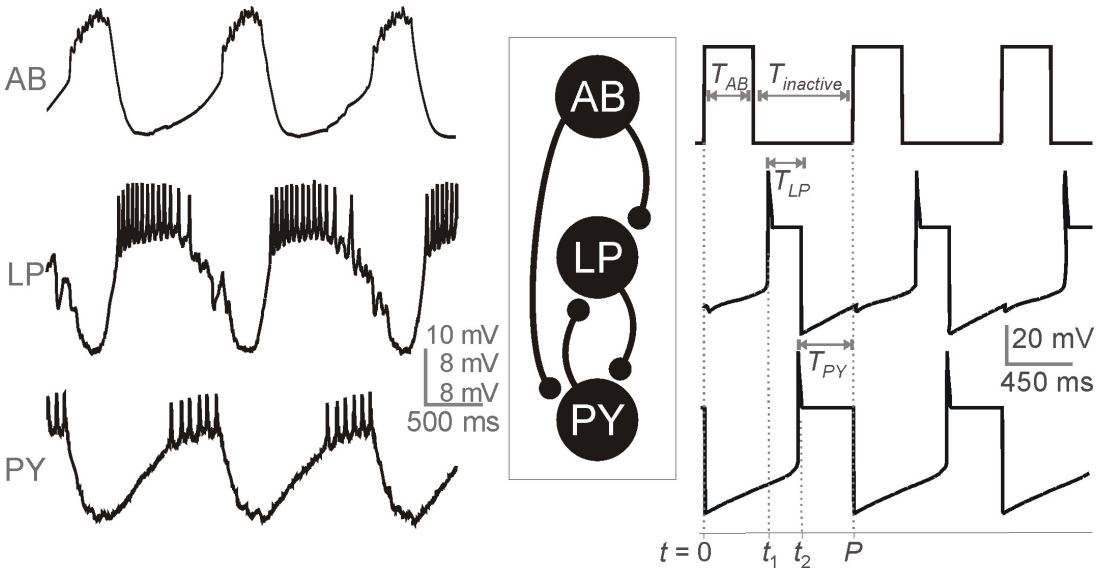

Fig. 1 Voltage traces of a typical ongoing tri-phasic pyloric rhythmic activity involving the pacemaker neuron *AB* and follower neurons *LP* and *PY*. Left traces show experimental recordings (Nadim, unpublished data) and the traces on the right are the simulation of our model which provides an approximation to the envelope of oscillations observed in the experimental traces. The temporal parameters are marked in the model traces. The middle panel is a reduced schematic diagram of the pyloric network, showing the cells and synapses used in the model.

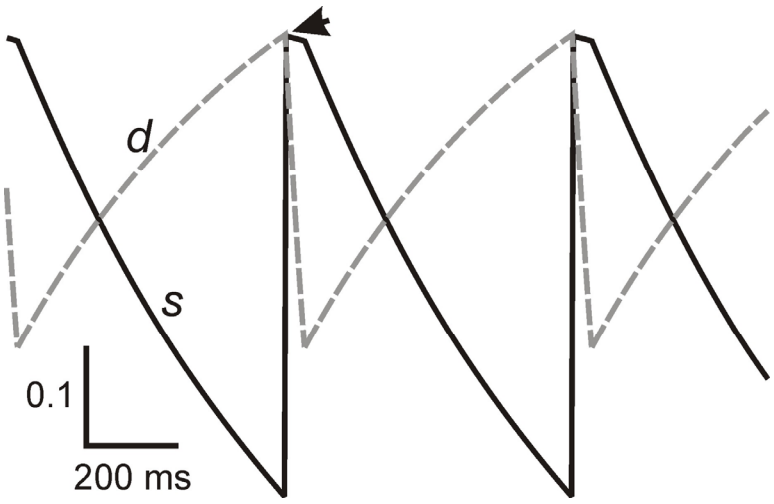

Fig. 2 Dynamics of the synaptic and depression variables. At the moment (marked by arrow) the presynaptic cell becomes active, the synaptic variable *s* (solid trace) is set to the current value of the variable *d* (dashed) that tracks depression and recovery. At all other times, the two variables are uncoupled and governed by distinct sets of equations.

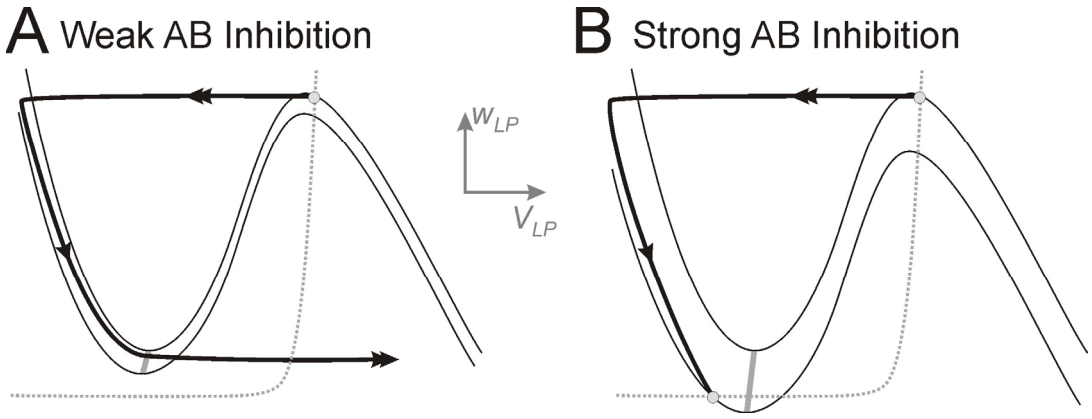

Fig. 3 The influence of *AB* inhibition on the dynamics of *LP*. **A.** The inhibition from *AB* to *LP* causes *LP* to return to the silent state, but is too weak to affect the time that *LP* spends in this state. Note the lack of intersection of the *v*- (solid) and *w*-nullclines (dotted) along the left branches. **B.** The inhibition from *AB* is strong and creates a fixed point on the left branch of the *v*-nullcline. In this case *LP* must wait for *AB* inhibition to decay, thereby allowing the stable fixed point (lower white circle) to disappear before it can jump to the active state. White circles indicate stable fixed points. The two *v*-nullclines in each case indicate no (upper) or maximal (lower) inhibition from *AB* to *LP*. The gray curve is the *LP* jump curve.

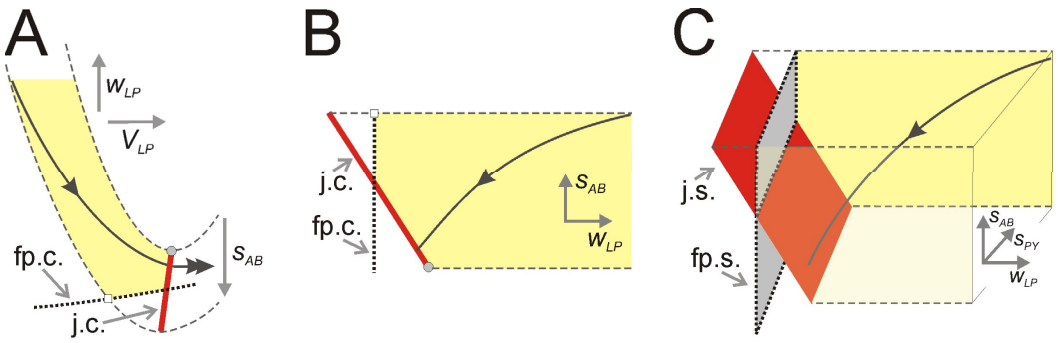

Fig. 4 Jump curves and surfaces. **A.** The dynamics of *LP* activity in response to *AB* inhibition alone. The set of local minima of the *v*-nullclines forms a one-dimensional jump curve *j.c.* The *v*-nullclines for different values of AB inhibition (s_{AB}) form a surface (shaded) that is bounded by two extremes (dashed) in each case indicate no (upper) or maximal (lower) inhibition from *AB* to *LP*. The *w*-nullcline is the dotted curve. The trajectory is shown as a solid curve. Additionally, the intersection of the *w*-nullcline with different *v*-nullclines forms a curve of fixed points, *fp.c.* **B.** The projection of the slow manifold (shaded) depicted in panel A onto the w_{LP}-s_{AB} phase space. **C.** The dynamics of *LP* activity in response to both *AB* and *PY* inhibition is shown in the w_{LP}-s_{AB}-s_{PY} phase space. As in the case shown in panel B, the *LP* trajectory enters this slow phase space on the upper right and leaves on the jump surface on the lower left, after the synaptic variables have mostly decayed. The jump and fixed-point surfaces, *j.s.* and *fp.s.*, are both two-dimensional in this case.

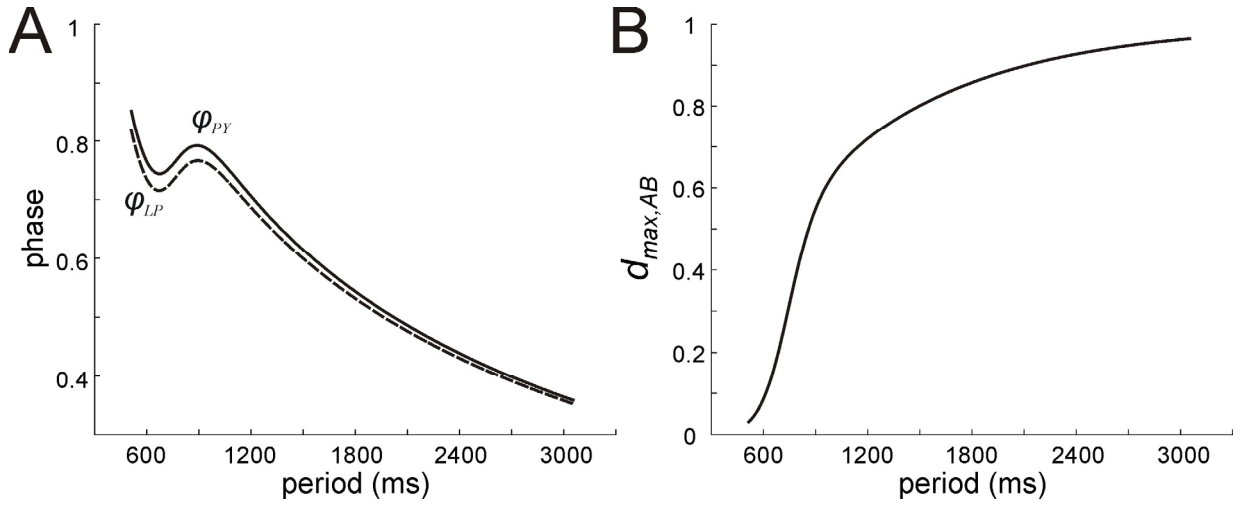

Fig. 5 Behavior of *LP* and *PY* when only *AB* inhibition is present. **A.** Phase curves for *LP* and *PY* show a stereotypical cubic shape indicating that different mechanisms and parameters control phase at different periods. **B.** The value of $d_{AB,max}$ increases with period. The strengthening of the feed-forward *AB* synapses for $P > 600$ causes the control of phase (as shown in panel A) to switch from the *LP* and *PY* intrinsic mechanisms to the AB synapses.

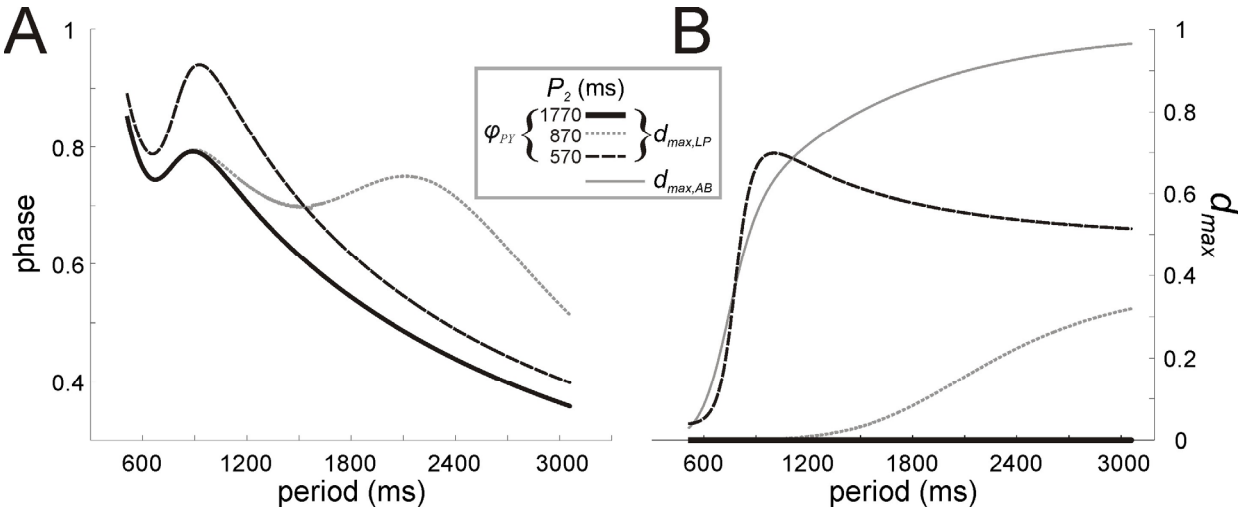

Fig. 6 Behavior of *PY* under *AB* and *LP* inhibition. **A.** The *PY* phase curves shown in three conditions indicate how the half-activation period (P_2) of the *LP* to *PY* synapse affects its ability to change the phase of *PY*. **B.** The behavior of $d_{LP,max}$ for the three cases shown in panel A. The value $d_{AB,max}$ (grey solid curve) is also shown to illustrate the relationship between the two synapses.

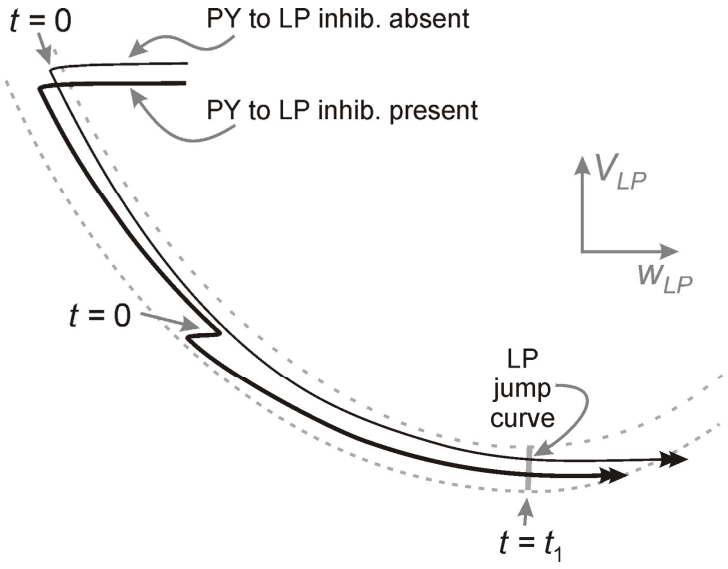

Fig. 7 The behavior of *LP* in the presence and absence of *PY* inhibition. Without *PY* inhibition, the time t_1 is calculated from the moment *LP* falls back to the silent state, associated with the onset of *AB* activity (t=0; top arrow) to the jump point. When *PY* inhibition is present (the bold trajectory), the onset of *AB* activity occurs at a lower point on the left branch of the v_{LP} nullcline (t=0; middle arrow) and t_1 is calculated from this moment to the jump point and is therefore much smaller.

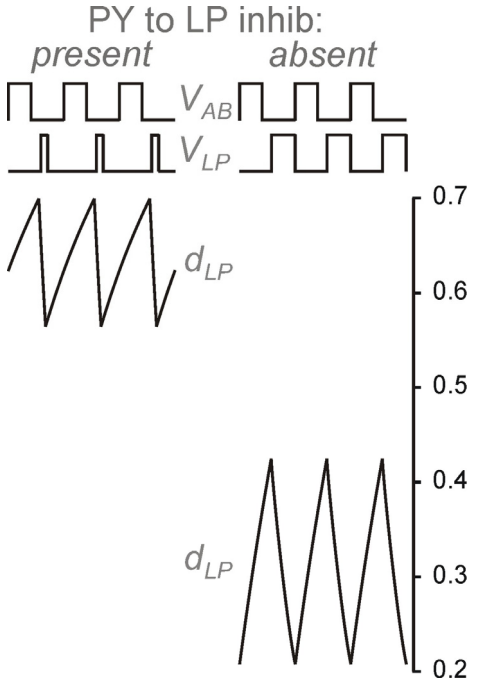

Fig. 8 The effect of *PY* inhibition on d_{LP}. When *PY* inhibition is present, *LP* inhibition strengthens independently of the half activation (P_2) of the synapse since *LP* spends more time in the silent state. When the *PY* inhibition is absent, the *LP* inhibition can only strengthen if P_2 is sufficiently small as *LP* spends relatively little time in the silent state.

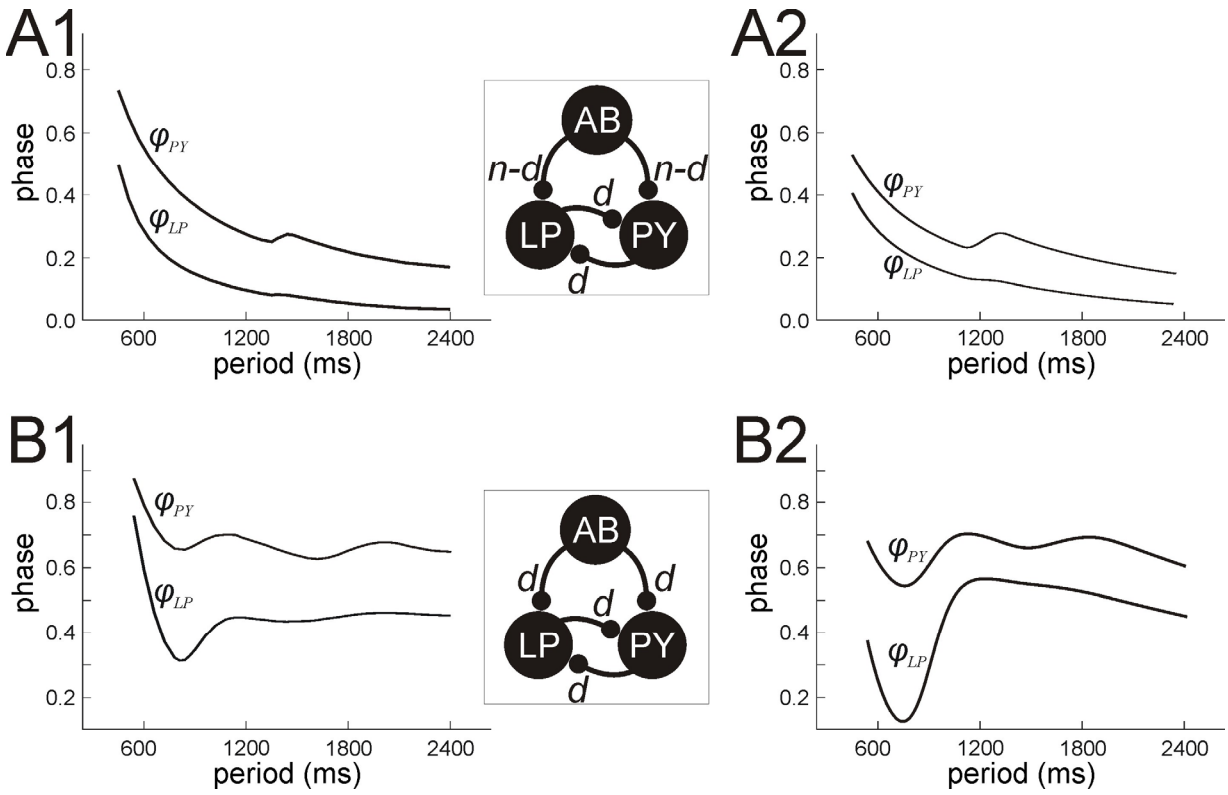

Fig. 9 *LP* and *PY* phase curves when reciprocal inhibition between the two is present. **A.** When the *AB* synapses are non-depressing, the *PY* phase can still be better than 1/*P* if the *LP* inhibition to *PY* is depressing. The local maxima of φ_{PY} are due to the strengthening of the *LP* to *PY* synapse. Also note the small increase in φ_{LP} near these periods. **B.** When the *AB* synapses are depressing, φ_{PY} and φ_{LP} can both have multiple local extrema. Panels A1 and B1 were obtained by numerically solving the full set of equations for their respective cases. Panels A2 and B2**,** obtained by solving equations (25) and (26), show good qualitative agreement with these numerical results.